The Erosion and Failure of the Volcanic Ash Slopes of Sakurajima

By Hidekazu MURATA* and Takumi OKABAYASHI**

(Received July 15, 1983)

Abstract

This paper reports the results of experimental investigation into the erosion and failure of the volcanic ash slopes. The major results obtained were: 1) The initial infiltration capacity of the volcanic ash layer is about 6×10^{-2}cm/sec, while the final capacity is between 5×10^{-4}cm/sec and 1×10^{-2}cm/sec. 2) With rainfall patterns which increase the water content gully erosion develops from the top of the slope. 3) High permeability of the lower parts of the slope contributes greatly to its stability. 4) Failure usually occurs when pore water pressure attains a constant value. 5) The conditions under which failure doesn't occur even though rainfall intensity exceeds infiltration capacity and causes runoff.

Introduction

Since the volcanic activity of Mt. Sakurajima resumed in 1955, calamitous mud slides have occurred. The major factors contributing to these slope failures are a season of heavy rainfall and the nature of the ash deposits.

This paper describes the infiltration capacity of the volcanic ash deposits and the way in which volcanic ash slopes are eroded and fail under the rainfalls.

Environmental Damage as a Function of Eruptions and Rainfall

Figure 1 shows the relationship between eruptions and natural disaster. The number of eruptions and the volume of falling ash are directly proportional, while the volume of rainfall and the number of occurrences of debris flows are almost in proportion to each other. Erosion and failure are more remarkable on the steeper upper slopes of the mountain. The fruit orchards of the lower slopes of northern Sakurajima are damaged more by falling ash and noxious gasses than by mud slides. Near the top of Mt. Minamidake, the location of the active caldera, ash falls are heavy and there is little plant life.

Experimental Method and Sample

Figure 2 shows the equipment used in the experiments involving infiltration capacity. The shape and dimensions of slopes in the erosion and failure experiments

* Department of Construction Engineering
** Kagoshima Technical College, Hayato, Aira, Kagoshima

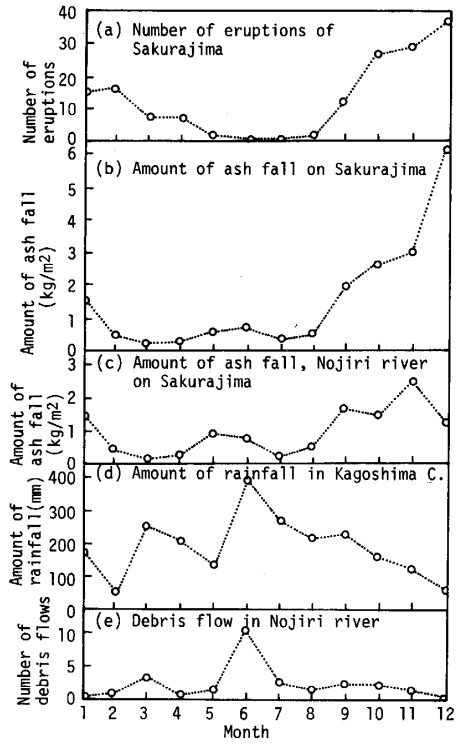

Fig. 1 Volcanic activity and natural disaster on Sakurajima.

are shown in Fig. 3. Rainfall can be set at any intensity from 40 to 1000 mm/h. Samples of volcanic ash were taken from the midslopes of the mountain. The ash samples have a maximum grain size of 10 mm, a specific gravity of particle of 2.50, a coefficient of permeability of 1.1×10^{-2} cm/sec ($\rho_t = 1.469$ g/cm^3) and maximum and minimum void ratios of 0.667 and 0.418. The sample contained 20% gravel, 75% sand, and 5% silt. Table 1 shows the experimental conditions.

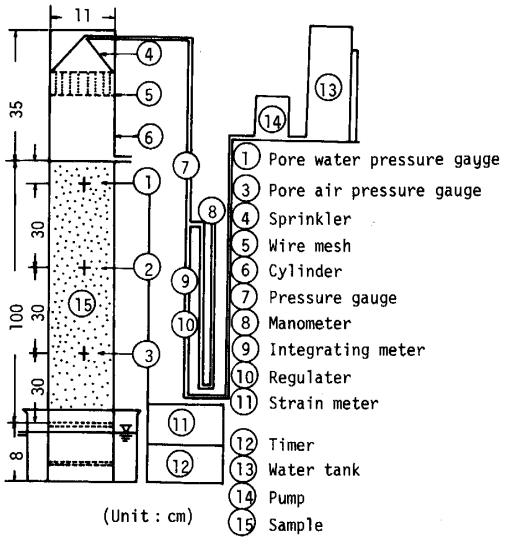

Fig. 2 Apparatus for infiltration capacity test.

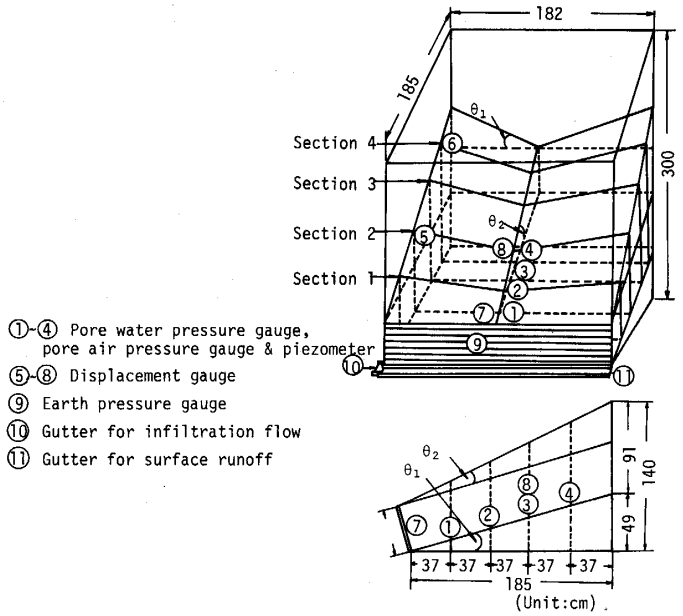

Fig. 3 Form and dimensions of experimental slope.

Infiltration Capacity

There are a number of important landmarks in the history of infiltration theory, beginning with Horton's first pointing[1] out the significance of the infiltration capacity of unsaturated soil under rainfall. This was followed by Philip's fundamental formula[2] for vertical infiltration, by Youngs & Peck's discussion[3] of the behavior of pore air pressure during the vertical penetration of rain water, and, more recently, by the work of Nisida et al.[4] with their application of the theory to the problem of slope stability. Insufficient attention, however, has been paid to the matter of infiltration velocities. The authors have published a study on the infiltration velocity of original Shirasu ground[5]. Horton showed that the following relationship between infiltration capacity, f_t, and rainfall time, t, is empirically true:

$$f_t = f_c + (f_0 - f_c)\, e^{-kt} \tag{1}$$

where, f_t = infiltration capacity (cm/sec), f_0 = initial infiltration capacity (cm/sec), f_c = final infiltration capacity (cm/sec), and k = a constant ($\sec^{-1}$).

Figure 4 shows the relation between infiltration capacity and rainfall time. Horton's equation is significant in describing the behavior of volcanic ash as the observed values are equal to the calculated ones. The initial infiltration capacity of the volcanic ash layer is about 6×10^{-2} cm/sec, while the final capacity is between 5×10^{-4} cm/sec and 1×10^{-2} cm/sec. The greater the rainfall, the more quickly infiltration capacity reaches a constant value.

Figure 5 shows the relation between surface runoff intensity and rainfall time. Surface runoff is:

$$f_s = r - f_t - f_{st} \tag{2}$$

Table 1. Experimental conditions.

Exp. No.	Rainfall intensity (mm/h)	Rainfall pattern (mm)	Slope angle	Base layer condition	Initial moisture content (%)	Wet density (g/cm^3)	Remarks column
20	821	1000	$\theta_1=\theta_2=\theta_3=0°$	Permeable layer	1.0	1.460	Infiltration capacity test
21	40	1000	"	"	1.0	1.460	"
1	80	150	$\theta_1=\theta_3=15°$, $\theta_2=0°$	Impermeable layer	5.4	1.470	Erosion and collapse test
2	96	120	"	"	8.9	1.790	"
3	96	1140	"	"	1.2	-	"
4	94	90	$\theta_1=\theta_2=\theta_3=15°$	"	6.7	1.760	"
5	96	131	"	"	5.5	1.710	"
6	86	93	"	"	7.6	1.400	"
7	80	131	"	"	5.6	1.470	"
8	80	115	"	"	8.6	1.360	"
9	63	138	"	"	5.7	1.470	"
10	45	245	"	"	4.1	1.540	"
11	63	820	"	Permeable layer	6.8	1.470	"
12	64 ↓↑ 80 ↓↑ 93 ↓↑ 104	116	"	Impermeable layer	6.7	1.470	"
13		113	"	"	5.7	1.470	"
14		105	"	"	-	-	"
15		102	"	"	6.0	1.470	"
16		80	"	"	7.4	1.370	"
17		50	"	"	8.5	-	"
18		205	"	"	8.5	1.380	"
19	39	340	"	"	8.2	1.450	"

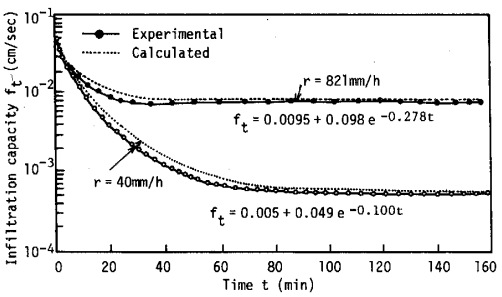

Fig. 4 Infiltration characteristics of ash fall.

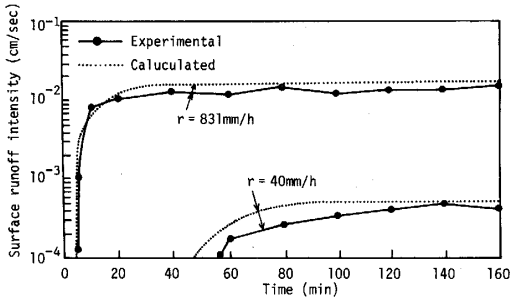

Fig. 5 Relation between surface runoff intensity and time.

where, f_s = surface runoff (cm/sec), r = rainfall intensity (cm/sec) and f_{st} = surface ponding intensity (cm/sec). As seen in Fig. 5, surface runoff intensity is inclined to approach a

steady value during rainfall. Surface runoff intensity tends to vary directy with rainfall, reaching a constant value of 50% with rainfall above 40 mm/h.

Water Behavior within the Slope

Figures 6(a) and (b) show experimental results during continuous rainfall. The piezometer water level shows a gradual increase from the top to the bottom of the slope. A feature of the equipment is that it separates the component of rainfall into three parts, filtration flow, surface runoff, and pore water. Unit surface runoff has a tendency to occur when unit filtration flow reaches an almost constant value. The final slope failure, during every rainfall, occurred after gully erosion began due to surface runoff. Even with the high rainfall characteristic of southern Kyushu, runoff does not occur until infiltration capacity is exceeded. Figure 7(a) elucidates the runoff characteristics of the slope after the termination of rainfall. Figure 7(b) is intended to show slope stability before the termination of rainfall. As seen in Fig. 7 unit infiltration flow and piezometer water level have a tendency to subside after rainfall stops and, with returning rainfall, to increase in proportion to rainfall intensity. Figure 7 is an example of experimentally generated infiltration flow and therefore is somewhat different from a natural and continuous rainfall pattern. One must consider also that the piezometer water level increases gradually during the repetition of a natural cycle of. rainfall so that the stability of the slope is a function of the duration and intensity of each period of rain as well as the spacing of the periods.

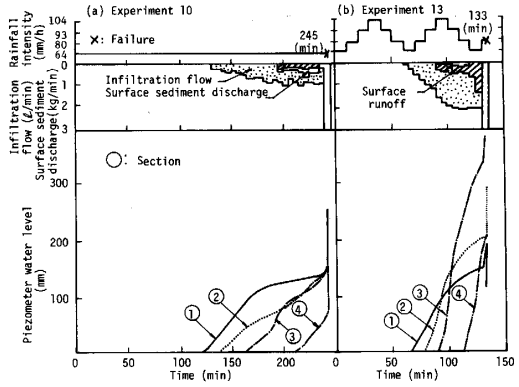

Fig. 6 Experimental results of continuous rainfall pattern.

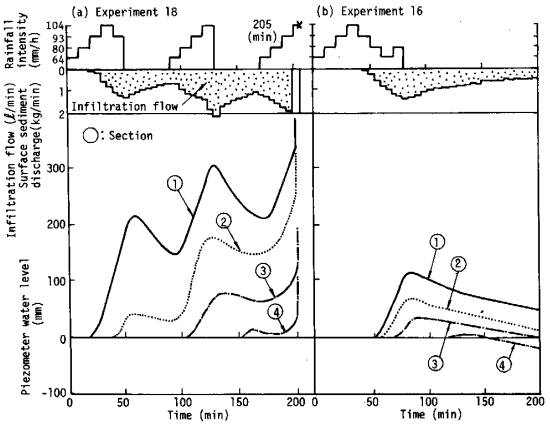

Fig. 7 Experimental results of intermittent rainfall patern.

Figure 8 (experiments 3 and 9) shows the results of varying slope, with $\theta_1=\theta_3=15°$, $\theta_2=0°$, and $\theta_1=\theta_2=\theta_3=15°$. Runoff at low angles occurs when the unit infiltration flow becomes steady at about 5.5 liters per minute. Unit surface sediment discharge varies directly with unit surface runoff. The piezometer water level reaches a steady state beginning at the top of the slope when the unit surface runoff becomes constant. This is true for small angles of inclination. For higher angles, as seen in Fig. 8(b),

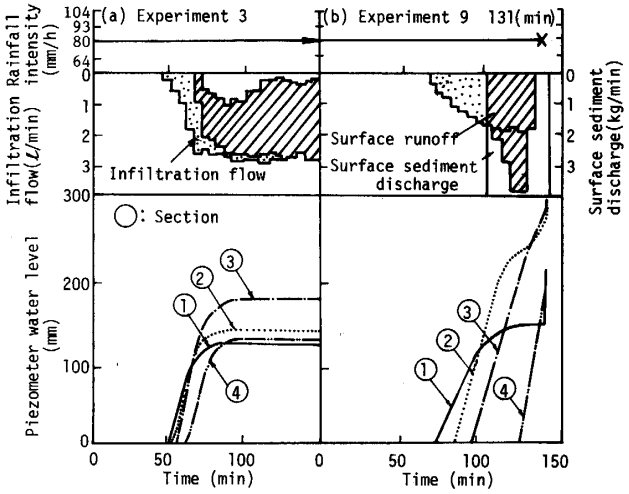

Fig. 8 Experimental results of varying angles of inclination.

this same condition results in collapse of the slope after gullies have developed.

Compared with higher angles, the relatively shallow slopes have difficulty attaining a steady state of the piezometer water level. Except for profile 1, slope failure occurs suddenly whenever piezometer water level increases rapidly. This suggests a limit to storage water for slopes with thin deposits of ash.

Figure 9 shows the velocity of stored water as a function of rainfall time for profile 2. For slopes of the same inclination the velocity of stored water depends on the drainage characteristics of the top of the slope. The storage velocity is first measurable shortly after the onset of the rain and increases rapidly until saturation at which time it falls rapidly. Furthermore, the higher the slope inclination, the less the storage velocity of the stored water. Figure 10 shows the relation between the piezometer water level and cumulative rainfall. The piezometer water levels of the high angle slopes of experiments

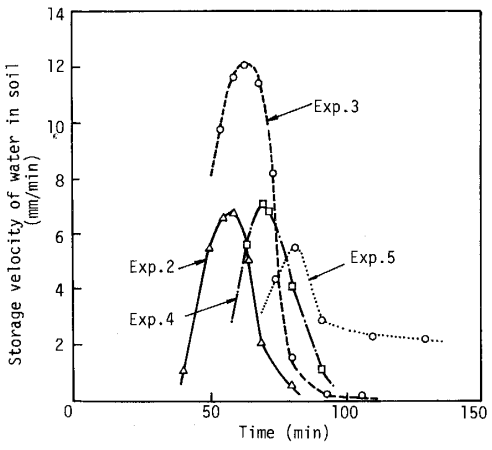

Fig. 9 Relation between storage velocity of water in soil and rainfall duration.

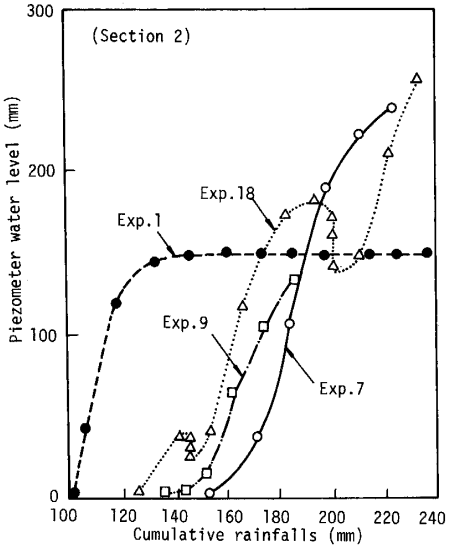

Fig. 10 Relation between piezometer water level and cumulative rainfalls.

7, 9, and 18 show that higher cumulative rainfalls are the results of higher rainfall intensities. Since the deeper layers of the slope are relatively impermeable, the seepage water per unit of rainfall is generally low. For the low angle slope of experiment 1, the relation between cumulative rainfall and piezometer water level tends to reach a steady state more quickly than it does for steeper slopes. This shows that the permeable layer is thin and easily saturated.

Figure 11 shows the distribution of pore water pressure in the ravines of the centrally located slopes. These are the results of experiments 6, 10, and 11 in which the rainfall is continual and of constant intensity. In experiment 11 there is a 50 mm permeable layer in the lower section of the slope. In experiments 6 and 10 the pore water pressure appears early and increases rapidly, particuraly toward the rear of the slope due to the high intensity of rainfall. In experiment 11, the pore water pressure reached only 0.2 kPa in section 1 for a rainfall intensity of 64 mm/h and after 370 minutes of rain. This was due to a high infiltration flow resulting from a sufficiently permeable drainage layer.

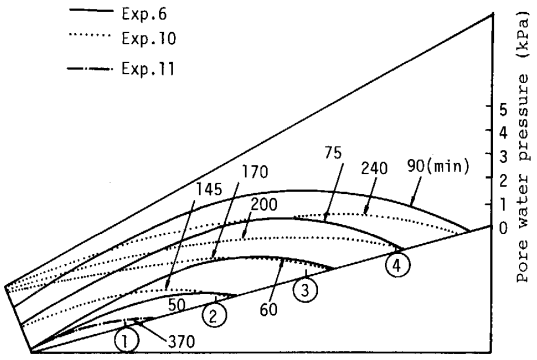

Fig. 11 Characteristics of pore water pressure in slope.

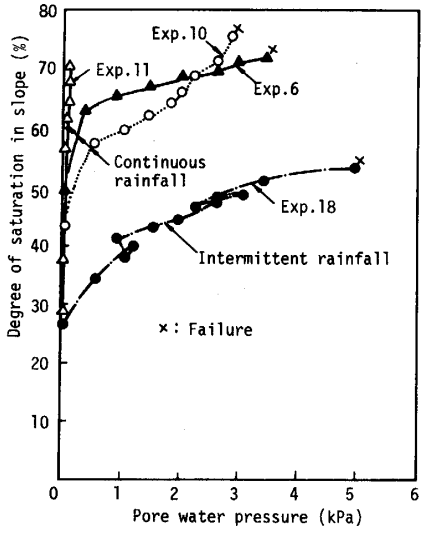

Fig. 12 Relation between degree of saturation and pore water pressure in slope.

Figure 12 shows the relation between the mean degree of saturation of the slope and pore water pressure for section 2 in a central slope area. As seen in Fig. 12, compared with the intermittent pattern of rainfall in experiments 6 and 11, the mean saturation is comparatively low at the moment of slope failure. This is due to the draining of storage water by seepage after the rain has stopped.

Characteristics of Erosion and Failure

As seen in Fig. 6, gully erosion occurred only during continuous rainfall. The course of such erosion is as follows: First, water begins to flow into the slope from the top. Secondly, after the gradual increase of this seepage, it reaches a constant value of

about 2 liters per minute. Then, surface runoff begins to occur, and with it, the movement of small particles. Particle movement induces the movement of series of particles, and this directs the flow into rivulets which increasingly localize fluid pressure and encourage deeper gully formation. As gullies becom deeper, they begin to develope their characteristically arborescent form. From this it can be seen that surface runoff occurs when rainfall intensity produces water in excess of the infiltration capacity. Gullies develop by the channelization and subsequent intensification of the surface runoff water pressure. Figure 13 shows the relation between pore water pressure and

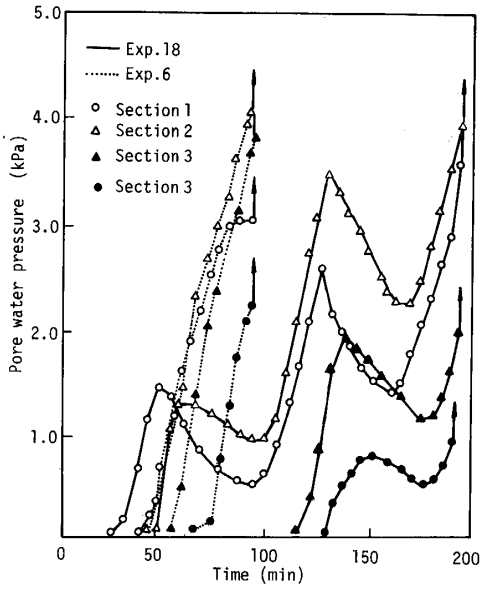

Fig. 13 Characteristics of pore water pressure under the rainfall.

rainfall duration for both a continuous pattern of rainfall, as in experiment 6, and an intermittent pattern, as in experiment 18. These show that every case of failure occurs when the pore water pressure at section 2 reaches 4 kPa. Experiment 18 shows that slope failure can occur if supplemental rainfall has prevented the complete drainage of water from the slope, even when the rainfall intensity is smaller than before. Inpredicting failure it is, therefore, necessary to give full consideration to what degree previous rainfall has contributed to the water content, and hence, the instability of the slope. Figure 14 shows the final failure curve of a slope and surface runoff for patterns of continuous rainfall. The time between the onset of surface runoff and slope failure is larger for smaller rainfall intensities. The rainfall intensity must, of course, exceed the infiltration capacity for runoff to occur.

Failure tends to occur early when the rainfall is particularly intense. Figure 14 allows the accurate prediction of the time of failure when the rainfall intensity is known. A rainfall intensity of about 25 mm/h seems to be critical, allowing saturation without failure. This value is the result of experimental techniques and must be corrected with actual data from the field.

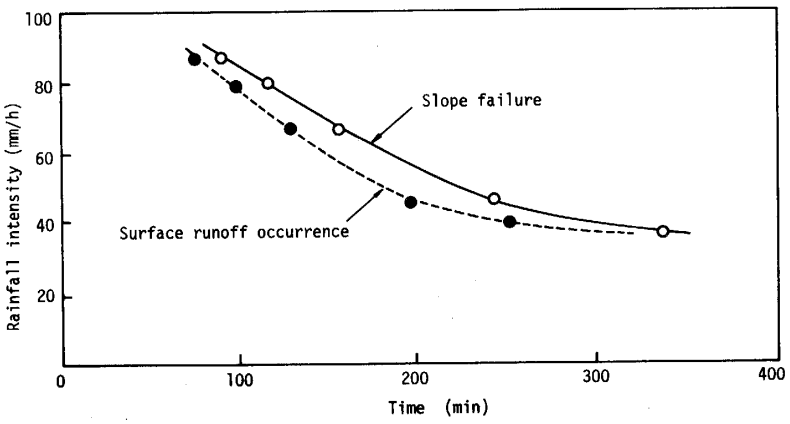

Fig. 14 Characteristics of slope failure.

Conclusions

The study of the failure of volcanic ash slopes under simulated rainfall patterns similar to those peculiar to southern Kyushu has led to a number of conclusions which offer some hope for understanding and predicting slope failure:

(1) During initial periods of rainfall the infiltration rate of volcanic ash deposits is on the order of 6×10^{-2} cm/sec with saturation the capacity falls to about 5×10^{-4} cm/sec but, in the case of intense rainfall, to only about 10^{-2}cm/sec. When rainfall is as great as 40 mm/h the surface runoff can be as high as 50%.

(2) Surface runoff intensity is directly proportional to rainfall intensity.

(3) Surface runoff occurs when rainfall exceeds infiltration capacity. Gully erosion starts at the top of the slope by the action of runoff water.

(4) The stored water in a slope decreases from the top to the bottom.

(5) Final slope failure occurs when pore water pressure reaches a constant value, The more intense the rainfall, the earlier this happens.

Acknowledgement

The authors wish to thank Professor Yamanouchi, Kyushu University, and Professor Kawaharada, Kagoshima University for their helpful advice.

This research was supported in part by a grant-in-aid for scientific research from the Ministry of Education, Science, and Culture.

References

1) Horton, R. E. "The Role of Infiltration in the Hydrogic Cycle", Trans. AGU., **14**, 446–460. (1933)
2) Philip, J. R. "The Theory of Infiltration", Soil Science, **83**, 345–357. (1957)
3) Youngs, E. G. and Peck, A. J. "Moisture Profil Development and Air Compression during Water Uptake bounded Porous Bodies", Soil Science, **98**, 290–294. (1965)

4) Nishida, Y., Yagi, N. and Futaki, M. "The Theoretical Analysis on the Pore Pressures due to Rain Water Permeation in the Ground', Proc. 6th Asian Regional Conf. SM & FE, **1**, 241–244, Singapore (1979)
5) Murata, H., Okabayashi, T. and Sayama, M. "Infiltration Capacity of Pumice Flow Soil "Shirasu" ", Proc. 7th Asian Regional Conf. SM & FE, Haifa, **1**, 342–345 (1983)